J|A|C|S
ARTICLES
Published on Web 03/16/2004

Density Functional Calculation of the 2D Potential Surface and Deuterium Isotope Effect on ^{13}C Chemical Shifts in Picolinic Acid *N*-Oxide. Comparison with Experiment

Jernej Stare,*,† Aneta Jezierska,†,‡ Gabriela Ambrožič,† Iztok J. Košir,†,§ Jurka Kidrič,† Aleksander Koll,‡ Janez Mavri,*,† and Dušan Hadži*,†

Contribution from the National Institute of Chemistry, Hajdrihova 19, SI-1000 Ljubljana, Slovenia, and Faculty of Chemistry, University of Wroclaw, F. Joliot-Curie 14, PL-50383 Wroclaw, Poland

Received November 11, 2002; Revised Manuscript Received March 19, 2003; E-mail: jernej@cmm.ki.si; janez@kihp2.ki.si; dusan.hadzi@ki.si

Abstract: 2D free energy surfaces $V = V(r_{OH}, r_{O\cdots O})$ for the intramolecular H-bond in the title compound were calculated by the DFT method and used in the calculation of primary and secondary chemical shifts of the compound dissolved in chloroform and acetonitrile. Solvent effects were accounted for by the SCRF/PCM method. The corresponding two-dimensional chemical shift surfaces with included solvent reaction field were obtained using the Continuous Set of Gauge Transformations approach at the B3LYP/6-311+G(2d,2p) level of theory. The chemical shifts were estimated as quantum averages along the two internal coordinates in the hydrogen bond and along several vibrational levels according to the Boltzmann distribution at room temperature. Fairly good agreement between the experimental and calculated isotope effects was obtained. 1D and 2D NMR spectra of solutions of picolinic acid *N*-oxide and its deuterated analogue were recorded and assigned.

1. Introduction

Among the most important applications of calculating molecular responses to external magnetic fields is the prediction of chemical shifts. It assists the interpretation of the NMR spectra of complex organic compounds and, in the case of short hydrogen bonding, the interpretation of isotope effects originating in the peculiar proton dynamics as governed by the effective potential surfaces.[1]

The theoretical treatment of the isotope effect including both the primary and secondary effects puts fairly high demands on the calculation of the two components of the procedure. The first is the plain computation of the chemical shifts that is a more general, by now well elaborated task,[2] and the second is the calculation of the Born−Oppenheimer surface. The quest for reliable potential surfaces and the thereupon dependent proton dynamics has been recently boosted by the widely discussed Cleland−Kreevoy proposal that considers the role of the strong, low barrier hydrogen bonds (SSHB, LBHB) in the energetics of important enzymatic reactions.[3] The arguments in support of the proposal and those refuting it include experimental and theoretical work.[4−13] In particular, in a very recent paper, evidence for the part played by an SSHB in the chymotrypsin mechanism has been drawn from the hydrogen/tritium NMR isotope shifts.[14]

Most of the experimental work and theoretical treatments of isotope effects on chemical shifts have been carried out on intramolecular hydrogen bonds.[1,15−17] This type of bonding is best suited for investigating the isotope effects because of the absence of complicating reflections of rotational isomerism and association equilibria. However, in the studies concerning hydrogen bonds, both the temperature[18] and solvent effects have to be taken into account. The latter may quite strongly affect the proton dynamics, and this effect is of major importance for proton dynamics dependent biochemical processes.

† National Institute of Chemistry.
‡ University of Wroclaw.
§ Present address: Institute of Hops Research and Brewing of Slovenia, Žalskega tabora 2, SI-3310 Žalec, Slovenia.

(1) Altman, L. J.; Laungani, D.; Gunnarsson, G.; Wennerström, H.; Forsén, S. *J. Am. Chem. Soc.* **1978**, *100*, 8264−8266.
(2) Gregor, T.; Mauri, F.; Car, R. *J. Chem. Phys.* **1999**, *111*, 1815−1822.
(3) Cleland, W. W.; Kreevoy, M. M. *Science* **1994**, *264*, 1887−1890.
(4) Warshel, A.; Papazyan, A.; Kollman, P. A. *Science* **1994**, *269*, 102−104.
(5) Schwartz, B.; Drueckhammer, D. G. *J. Am. Chem. Soc.* **1995**, *117*, 11902−11905.
(6) Mulholland, A. J.; Lyne, P. D.; Karplus, M. *J. Am. Chem. Soc.* **2000**, *122*, 534−535.
(7) Zhao, Q.; Abeygunawardana, C.; Talalay, P.; Mildvan, A. S. *Proc. Natl. Acad. Sci. U.S.A.* **1996**, *93*, 8220−8224.
(8) Viragh, C.; Harris, T.; Reddy, P.; Massiah, M.; Mildvan, A. S.; Kovach, I. *Biochemistry* **2000**, *39*(51), 16200−16205.
(9) Frey, P. A.; Whitt, S. A.; Tobin, J. B. *Science* **1994**, *264*, 1927−1930.
(10) Shan, S.; Loh, S.; Herschlag, D. *Science* **1996**, *272*, 97−101.
(11) Shan, S.; Herschlag, D. *J. Am. Chem. Soc.* **1996**, *118*, 5515−5518.
(12) Kato, Y.; Toledo, L. M.; Rebek, J., Jr. *J. Am. Chem. Soc.* **1996**, *118*, 8575−8579.
(13) Helgaker, T.; Jaszunski, M.; Rund, K. *Chem. Rev.* **1999**, *99*, 293−352.
(14) Westler, W. M.; Frey, P. A.; Lin, J.; Wemmer, D. E.; Morimoto, H.; Williams, P. G.; Markley, J. L. *J. Am. Chem. Soc.* **2002**, *124*, 4196−4197.
(15) Hansen, P. E. *Annu. Rep. NMR Spectrosc.* **1983**, *15*, 105.
(16) Perrin, C. L. *Science* **1994**, *266*, 1665−1668.
(17) Dziembowska, T.; Rozwadowski, Z.; Hansen, P. E. *J. Mol. Struct.* **1997**, *436*−*437*, 189−199.
(18) Garcia-Viloca, M.; Gelabert, R.; Gonzalez-Lafont, A.; Moreno, M.; Lluch, J. M. *J. Am. Chem. Soc.* **1998**, *120*, 10203−10209.

10.1021/ja021345f CCC: $27.50

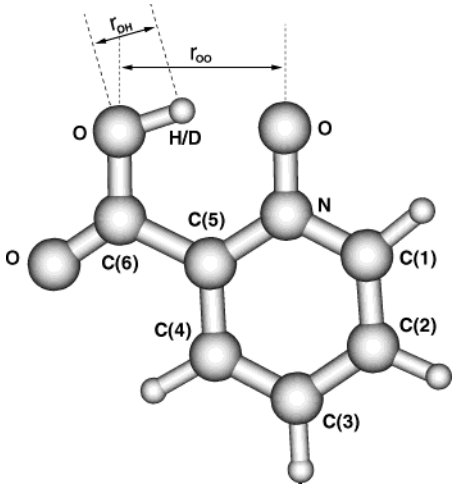

Figure 1. Structure and atom numeration of picolinic acid *N*-oxide (PANO).

The quality of the theoretical treatments of NMR isotope effects is thus dependent upon the ability to account for the responses to external magnetic fields and in computations of realistic potential surfaces. To our knowledge, one-dimensional (1D) proton potential functions were so far used for this purpose.[19,20] For qualitative interpretations of the isotope effects, it is quite adequate to use the schematic division of the potential function into asymmetric, centered symmetric and double minimum type functions. For quantitative treatment of isotope effects, it is likely that at least two-dimensional functions are required. It is well-known that, for the reproduction of vibrational spectra, accounting for anharmonic coupling between the high and low-frequency stretchings of the hydrogen bond is mandatory.[21,22]

In this paper, we present the results of calculations on the example of picolinic acid *N*-oxide (PANO) (see Figure 1). This compound was chosen because it contains a fairly short, slightly asymmetric intramolecular hydrogen bond (2.425 Å in the crystal, ref 23) that is sensitive to solvent effects as shown by the infrared spectra and well reproduced by calculations of the 1D potential function.[24] For the present study, 2D potential functions were calculated along the O−H and O···O coordinates using the density functional theory. To account for the solvent effect, the SCRF/PCM method of Tomasi and co-workers[25,26] was applied. Two solvents of differing permittivities were adopted, i.e., chloroform ($\epsilon = 4.9$) and acetonitrile ($\epsilon = 36.5$). Experimental data were acquired for comparison with the theoretical results.

The outline of this article is the following: in sections 2 and 3 are given the details of the experimental and computational work, respectively, followed by the results of the computations and discussion in section 4. Concluding remarks are presented in section 5.

2. Experimental Section

Sampling. Commercial (Aldrich) PANO was purified by recrystallization from aqueous methanol. Deuterated PANO was prepared by recrystallization from methanol-d_1/D_2O mixtures. Solvents were of spectroscopic grade. For the ^{1}H PANO, CD_3CN (CIL) and $CDCl_3$ (CIL) were used as solvents and TMS (CIL) was added. For the acquisition of PANO-d_1 spectra, CH_3CN and $CHCl_3$ (Merck) solvents were used. Hexafluorobenzene (Aldrich) was added for the lock signal (^{19}F), and $CDCl_3$ was used as the internal chemical shift standard.

NMR Spectroscopy. The NMR spectra were recorded on a Varian UNITY$^+$ 300 NMR spectrometer. The spectrometer was equipped with a 10.0 mm broad band probe, operating at 299.860 MHz for ^{1}H and 75.408 MHz for ^{13}C. For one-dimensional ^{1}H spectra, 64 transients were accumulated with 62 272 data points over a 7000.4 Hz bandwidth. ^{13}C spectra were acquired with 60 224 data points over a 20 000.0 Hz bandwidth with a 22.0 μs (45°) radio frequency pulse. The number of transients was 24 000, with the delay of 10 s between scans.

For recording the ^{2}H spectra, the spectrometer was equipped with a 10.0 mm probe with a fluorine lock, operating at a ^{2}H frequency of 46.031 MHz. For each spectrum, 64 transients were accumulated with 16 320 data points over a 1200.0 Hz spectral bandwidth with a 20.0 μs (90°) rf pulse and proton decoupling (WALZ).

Two-dimensional NMR spectra COSY, HSQC, and HMQC were recorded on a Varian INOVA-600 NMR spectrometer. Both instruments are located at the NIC (Slovenian National NMR Centre, Ljubljana). The 600 MHz instrument was equipped with a 5.00 mm Indirect Detection Pulsed Field Gradients probe (ID-PFG), operating at a ^{1}H frequency of 600.126 and 150.914 MHz for ^{13}C.

Two-dimensional homonuclear COSY experiments were acquired with 4096 data points covering a spectral width of 15 000.9 Hz. 64 scans were acquired for each of the 512 increments. Two-dimensional heteronuclear HSQC spectra were acquired with a relaxation delay of 1.5 s between scans, and GARP decoupling was applied during acquisition. 64 scans with 2048 data points were acquired for each of the 512 increments covering a spectral width of 10 400.7 Hz in F2 and 30 007.5 Hz in F1 dimension.

Two-dimensional heteronuclear long-range NMR spectra HMQC consisted of 1984 data points over a 14 000.7 Hz bandwidth. 64 scans were acquired for each of the 512 increments.

The assignment of all chemical shifts in PANO was performed with the use of 1D ^{1}H and ^{13}C NMR experiments and with 2D homo- and heteronuclear NMR experiments COSY, HSQC, and HMQC. Details of the analysis of spectra will be published together with those of two substituted (*p*-nitro, *p*-methoxy) picolinic acid *N*-oxides.

3. Computational

The potential energy and chemical shift surfaces were calculated using the *Gaussian 98* suite of programs.[27] In calculating the potential energy surface (PES), the O−H and O···O coordinates were fixed in steps, while the other degrees of freedom were optimized. The dihedral angles associated with the carboxylic group were kept frozen in order to retain planarity of the systems and to avoid undesired rotations of the carboxylic group. Each of the two potential energy surfaces consisted of about 140 points corresponding to different

(19) Munch, M.; Hansen, A. E.; Hansen, P. E.; Bouman, T. D. *Acta Chem. Scand.* **1992**, *46*, 1065−1071.
(20) Abildgaard, J.; Bolvig, S.; Hansen, P. E. *J. Am. Chem. Soc.* **1998**, *120*, 9063−9069.
(21) Sokolov, N. D. *Chem. Phys.* **1986**, *104*, 371−381.
(22) Henri-Rousseau, O.; Blaise, P. In *Theoretical Treatments of Hydrogen Bonding*; Hadži, D., Ed.; J. Wiley: Chichester, 1997; pp 165−186.
(23) Steiner, T.; Schreurs, A. M.; Kroon, M. L. J. *Acta Crystallogr.* **2000**, *C56*, 577−579.
(24) Stare, J.; Mavri, J.; Ambrožič, G.; Hadži, D. *THEOCHEM* **2000**, *500*, 429−440.
(25) Miertus, S.; Scrocco, E.; Tomasi, J. *Chem. Phys.* **1981**, *55*, 117.
(26) Tomasi, J.; Persico, M. *Chem. Rev.* **1994**, *94*, 2027−2094.
(27) Frisch, M. J.; Trucks, G. W.; Schlegel, H. B.; Scuseria, G. E.; Robb, M. A.; Cheeseman, J. R.; Zakrzewski, V. G.; J. A. Montgomery, J.; Stratmann, R. E.; Burant, J. C.; Dapprich, S.; Millam, J. M.; Daniels, A. D.; Kudin, K. N.; Strain, M. C.; Farkas, O.; Tomasi, J.; Barone, V.; Cossi, M.; Cammi, R.; Mennucci, B.; Pomelli, C.; Adamo, C.; Clifford, S.; Ochterski, J.; Petersson, G. A.; Ayala, P. Y.; Cui, Q.; Morokuma, K.; Malick, D. K.; Rabuck, A. D.; Raghavachari, K.; Foresman, J. B.; Cioslowski, J.; Ortiz, J. V.; Stefanov, B. B.; Liu, G.; Liashenko, A.; Piskorz, P.; Komaromi, I.; Gomperts, R.; Martin, R. L.; Fox, D. J.; Keith, T.; Al-Laham, M. A.; Peng, C. Y.; Nanayakkara, A.; Gonzalez, C.; Challacombe, M.; Gill, P. M. W.; Johnson, B.; Chen, W.; Wong, M. W.; Andres, J. L.; Gonzalez, C.; Head-Gordon, M.; Replogle, E. S.; Pople, J. A. *Gaussian 98*, revision A.7. Gaussian, Inc.: Pittsburgh, PA, 1998.

values of O−H and O···O distances. Several basis sets (6-31G(d), 6-31+G(d,p), 6-31+G(2d,2p), 6-311+G(d,p), 6-311+G(2d,2p), and 6-311++G(3df,3pd)) were explored with the B3LYP functional. Finally, the 6-31+G(d,p) basis set was adopted as the best compromise between the quality of results and economy. For introducing the solvent effects, the SCRF/PCM model was applied. Two solvents were included in our calculations, chloroform ($\epsilon = 4.9$) and acetonitrile ($\epsilon = 36.5$).

Next, the chemical shift surfaces were calculated using the geometries obtained in the calculation of potential energy surfaces. The CSGT approach[28,29] and the SCRF/IEFPCM[30,31] methods in conjunction with the B3LYP/6-311+G(2d,2p) level of theory were used. (For recent advances in calculations of magnetic properties with included solvent reaction field, see Menucci and coworkers.[32,33])The corresponding solvent parameters were used with each of the two sets of structures, one set corresponding to chloroform and the other to acetonitrile. Note that the output of such calculations includes chemical shifts for all the nuclei in the molecule. The B3LYP/6-311+G(2d,2p) chemical shifts were also calculated for the B3LYP/6-31+G(d,p) geometry optimized structure of tetramethylsilane (TMS), which serves as a reference standard both in theoretical and experimental work. The chemical shift surfaces of PANO were recalculated relative to TMS. There were seven surfaces subjected to further calculations: the hydrogen of the H-bonded proton and six ^{13}C surfaces of the ring and the carboxylic carbon nuclei.

The pointwise represented surfaces were then subjected to fitting in order to get a suitable and computationally inexpensive form for further calculations. Free energy surfaces in chloroform and acetonitrile were represented as linear combinations of 24 and 11 Gaussian functions, respectively. The Gaussians were superimposed on a "hard core ceiling" of constant values of 200.00 and 293.67 kcal/mol, respectively, to ensure proper asymptotic behavior of the potential. Note that there is no significant difference in the shape of the chemical shift surface of a given nucleus between the solvents.

With suitable forms of PES, the two-dimensional vibrational Schrödinger equation (SE) was solved by the variational principle using a program, developed in our laboratory.[34] For solving the SE, a rectangular basis set of local constants was used,[35,36] spanning from 0.70 to 2.30 Å in the O−H direction with 32 intervals and from 2.00 to 3.40 Å in the O···O direction with 46 intervals; the total number of vibrational basis functions was thus $32 \times 46 = 1472$. The SE was solved for the proton (reduced mass of 1 au) and the deuteron (2 au) of the hydrogen bond. The reduced mass associated with the O···O coordinate was set to 20 au in order to reproduce the O···O stretching frequency, calculated within the harmonic approximation at the B3LYP/6-31+G(d,p) level.

After solving the SE, the resulting eigenfunctions were used to calculate the expectation values of the chemical shift functions of the considered nuclei according to the following expression:

$$\delta_k = \int\int \psi_k(x, y)\delta(x, y)\psi_k(x, y)\mathrm{d}x\,\mathrm{d}y$$

where δ_k is the chemical shift expectation value for the k-th vibrational level, $\delta(x, y)$ is the chemical shift function, obtained by fitting, and $\psi_k(x, y)$ is the wave function of the k-th vibrational level, obtained by solving the vibrational SE. Both functions are two-dimensional; hence x and y represent the O−H and O···O stretching coordinates, respectively. Since each of the resulting vibrational levels has its own wave function $\psi_k(x, y)$ and, consequently, its own expectation value δ_k, a Boltzmann-weighted averaging was performed over all vibrational levels:

$$\langle\delta\rangle_T = \sum_k \delta_k P_T(k)$$

$\langle\delta\rangle_T$ being the thermally averaged expectation value of the chemical shift at a given temperature T. $P_T(k)$ is the relative population of the k-th vibrational state at that temperature, according to the Boltzmann distribution and being equal to

$$P_T(k) = \frac{e^{-E_k/kT}}{\sum_k e^{-E_k/kT}}$$

where E_k is the energy of the k-th vibrational level. In our calculations, thermal averaging was performed only along the lowest 20 values; the temperature was set to 298 K (the population of higher levels is evidently negligible at this temperature; hence they can be left out in our calculations). The thermally averaged chemical shifts of the H-bonded proton and all the carbon nuclei of PANO were estimated in this way. The secondary isotopic effect was calculated as a difference between the thermally averaged expectation values obtained by the proton and deuteron wave function.

The calculations were performed on a cluster of 24 dual-CPU PC/Linux machines (AMD Athlon XP 1600+ model; 512 MB RAM each). The estimated single-processor time was about 7000 hours.

4. Results and Discussion

Absolute Values of the Chemical Shifts and the Isotope Effect. Potential energy surfaces, computed for each solvent, are shown in Figure 2. The chemical shift surfaces were expressed as two-dimensional polynomials of fifth or sixth degree, with all possible cross terms included. The chemical shift surfaces in chloroform are shown in Figures 3 and 4.

Table 1 lists the calculated and experimental chemical shifts of selected nuclei in PANO. With few exceptions, the calculations based on the quantum averaging of chemical shift functions are in better agreement with the experimental values than the plain calculations using the optimized geometry. In particular, the chemical shifts of the H-bonded hydrogen/deuterium match well the experimental values. There are larger discrepancies between the calculated and the experimental values for the ^{13}C chemical shifts; interestingly, the calculated values exceed as a rule the experimental ones by about 6−7%, suggesting a systematic error in the applied computational model that could be corrected by scaling for practical purposes.

Secondary isotope effects originate in the electronic coupling of the proton/deuteron vibrational wave function to the rest of the system. Namely, the differences in the geometry of the O−H(D)···O moiety slightly affect the geometry of the rest of the systems as well as the local electron density at the nuclei. In Table 2 are listed the calculated and experimental isotope effects. The secondary isotope effects are in general smaller than the primary one; their agreement with the experiment is somewhat worse than that of the primary isotope effect. Nevertheless, the calculations correctly predict the sign as well as the relative magnitude of secondary isotope effects at the carbon nuclei.

(28) Keith, T. A.; Bader, R. F. W. *Chem. Phys. Lett.* **1993**, *210*, 223−231.
(29) Cheeseman, J. R.; Trucks, G. W.; Keith, T. A.; Frisch, M. J. *J. Chem. Phys.* **1996**, *104*, 5497−5509.
(30) Cances, E.; Mennucci, B.; Tomasi, J. *J. Chem. Phys.* **1997**, *107*, 3032−3041.
(31) Tomasi, J. Private communication.
(32) Menucci, B.; Martinez, J. M.; Tomasi, J. *J. Phys. Chem. A* **2001**, *105*, 7287−7296.
(33) Menucci, B. *J. Am. Chem. Soc.* **2002**, *124*, 1506−1515.
(34) Stare, J.; Mavri, J. *Comput. Phys. Commun.* **2002**, *143*, 222−240.
(35) Marston, C. C.; Balint-Kurti, G. G. *J. Chem. Phys.* **1989**, *91*, 3571−3576.
(36) Balint-Kurti, G. G.; Dixon, R. N.; Marston, C. C. *Int. Rev. Phys. Chem.* **1992**, *11*, 317−344.

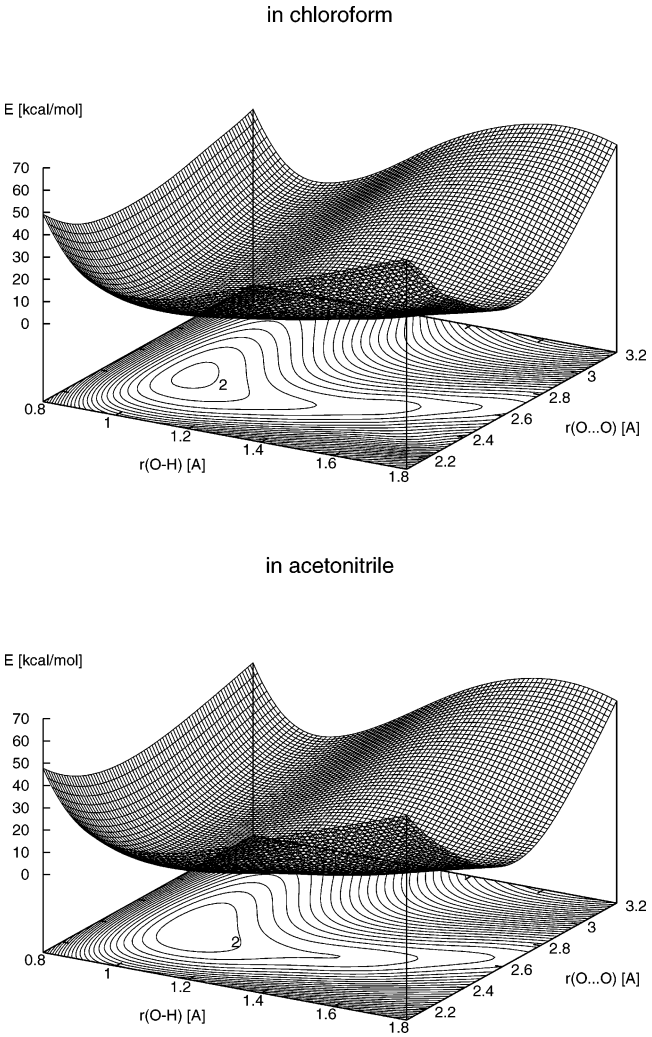

Figure 2. Potential energy surfaces of PANO in chloroform (top) and in acetonitrile (bottom). In both surfaces, the inner contour labeled "2" pertains to the energy value of 2 kcal/mol above the minimum; successive contours are drawn at 2 kcal/mol intervals.

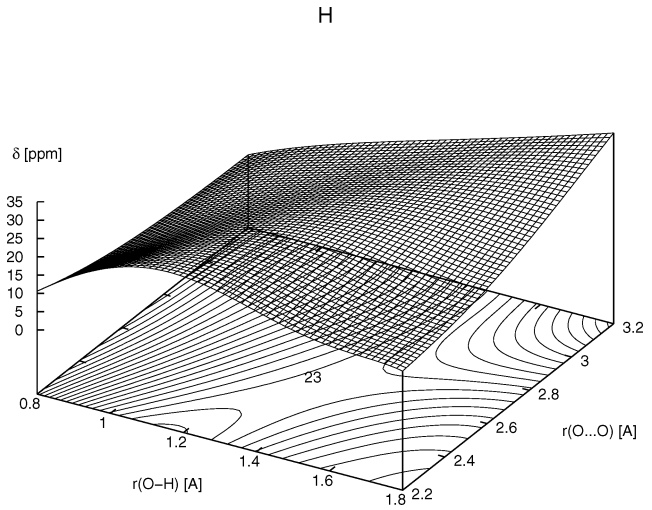

Figure 3. Chemical shift surface of the H-bonded hydrogen in PANO in chloroform. The resolution of the contours is 1 ppm; a contour pertaining to 23 ppm is labeled.

Solvent Effect. The differences between the chemical shifts depending on the solvent can be readily explained by the change in the free energy hypersurface and in the resulting positions of the nuclei. Moreover, as the solvent polarizes the electron wave function, the change of solvent polarity affects the electron density distribution in the molecule, giving rise to changes of shielding tensors of the nuclei. It is thus evident that acetonitrile, which is more polar than chloroform, affects the shape of the PES in that the energies of structures with high dipole moments are lowered, thus displacing the proton toward the *N*-oxide site and extending the O−H distance (see Figure 2). This effectively reduces the electron density at the hydrogen nucleus; therefore its chemical shift increases upon the replacement of chloroform by acetonitrile as solvent. The solvent effects are listed in Table 3. Similarly to the absolute values, the quantum averaging method yields, with only minor exceptions, better agreements with the experiment; in particular, this is the case for the H-bonded hydron. Interestingly, the relative magnitude of the solvent substitution effect is well predicted by calculations; however, the calculated values are about 0.9 ppm too small in most cases, suggesting a systematic error of the computational method. Again, the best agreement between calculations and experiment is achieved for the hydrogen bound hydron.

It is interesting to compare the primary isotope effect $\delta_H - \delta_D$ in PANO with some related examples of short, intramolecular hydrogen bonding and with independent experimental and theoretical evidence for the potential. The $\delta_H - \delta_D$ value of approximately 0.5 ppm corresponds fairly closely to the value obtained by experiments for quinaldic acid *N*-oxide;[17] the latter compound displays very similar metrics[23] of the hydrogen bond, and it may be expected that the similarity persists in solution. The infrared spectra support this expectation.[24] In both compounds, the X-ray diffraction shows the proton to be nearer to the carboxylic oxygen. Diverse examples of $\delta_H - \delta_D$ in short intramolecular H-bonds are collected in the seminal paper of Forsén and co-workers.[1] The ^{1}H chemical shifts and isotope effects of enolic β-diketones are comparable to those in PANO. Interestingly, the O ···O distances in the enolized diketones are longer than with PANO, but the calculated one-dimensional potential functions of the former are strongly anharmonic with low barriers. Incidentally, a similar isotope effect ($\delta H - \delta D \approx$ 0.7 ppm) was also obtained in an example of the intermolecular bonding which is the complex of pyridine and acetic acid.[37]

Comment on the Level of Theory. We were using the popular Becke's three-parameter hybrid exchange functional coupled with the Lee−Yang−Parr correlation functional,[38,39] dubbed B3LYP. We tested a fairly large number of basis sets and found 6-31+G(d,p) to be a good compromise between performance and quality of the resulting optimized structures and harmonic vibrational frequencies. We then chose the latter level for calculating the potential energy surfaces. Since all the gauge-independent methods require in general large and flexible basis sets (triple-ζ is usually recommended),[40] we chose B3LYP/6-311-G(2d,2p) for the calculation of chemical shift surfaces. The dependence of the single-point calculated chemical shifts on the basis set size in PANO is displayed in Figure 5. Note that even the largest basis sets exhibit a considerable difference

(37) Smirnov, S. N.; Golubev, N. S.; Denisov, G. S.; Benedict, H.; Schah-Mohammedi, P.; Limbach, H.-H. *J. Am. Chem. Soc.* **1996**, *118*, 4094−4101.
(38) Lee, C.; Yang, W.; Parr, R. G. *Phys. Rev. B* **1988**, *37*, 785−789.
(39) Becke, A. D. *J. Chem. Phys.* **1993**, *98*, 5648−5652.
(40) Hinton, J. F.; Wolinski, K. In *Theoretical Treatments of Hydrogen Bonding*; Hadži, D., Ed.; J. Wiley: Chichester, 1997; pp 75−93.

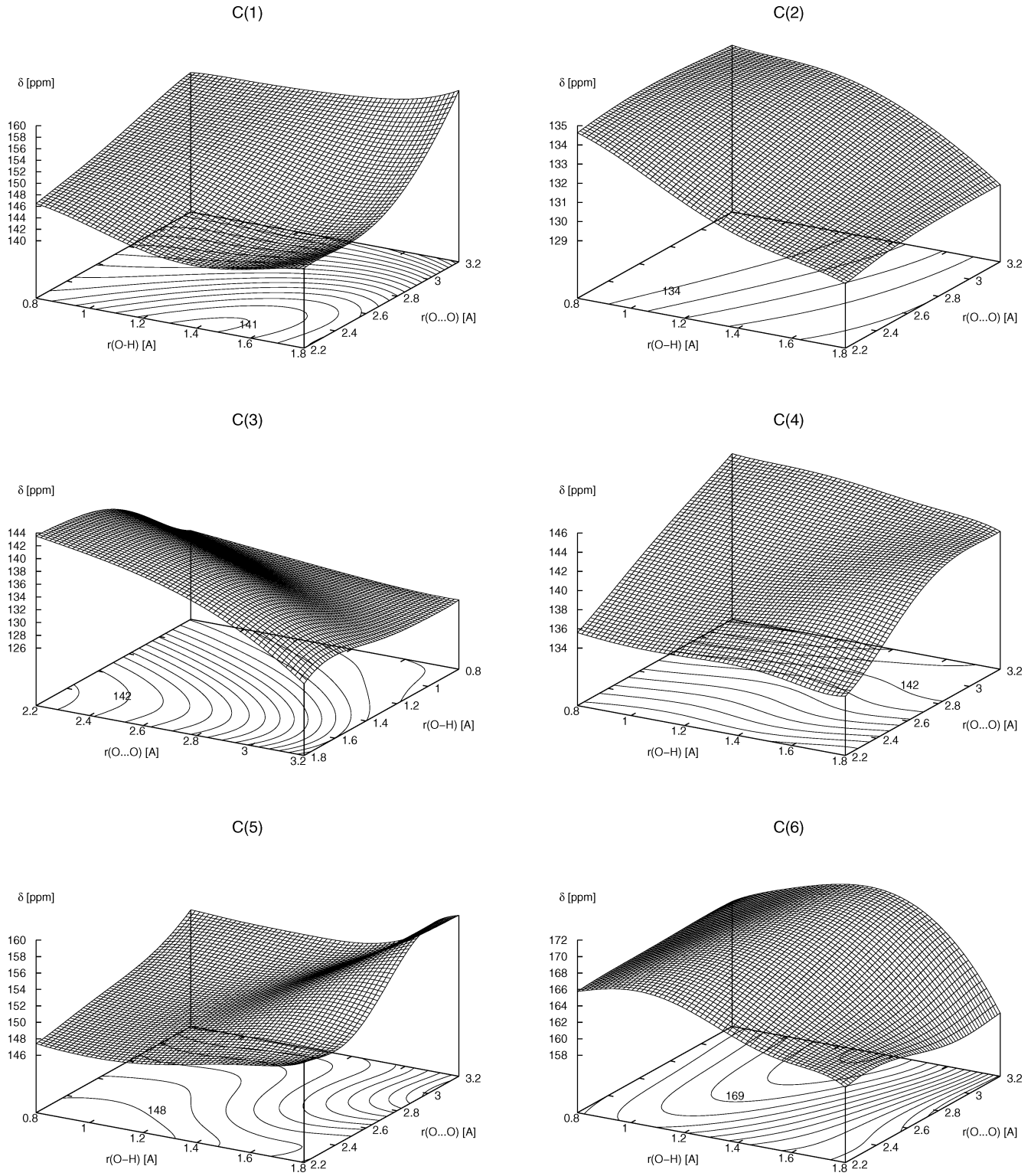

Figure 4. Chemical shift surfaces of the carbon nuclei in PANO in chloroform. The contour resolution is 1 ppm; for each nucleus, one of the contours is labeled according to its value in ppm.

between the calculated and measured chemical shifts. The discrepancy can be attributed to (i) inconsistencies of the model (gas phase calculations vs experiment in solution), (ii) limitations of the B3LYP functional, and (iii) lack of the quantum treatment of the nuclei, in particular the H-bonded hydrogen. For the latter, the chemical shift calculated at the B3LYP/6-311+G(2d,2p) level (SCRF/IEFPCM; chloroform) is 15.299 ppm in the fully geometry-optimized structure at B3LYP/6-311+G(d,p) (SCRF/PCM; chloroform). This value becomes 18.497 ppm after quantum averaging of the chemical shift surface, comparable to the experimental value 17.895 ppm in chloroform solution (see Table 1). This supports the initially stressed necessity of including the quantum treatment and anharmonicity of the O−H···O moiety in calculations. The quantum treatment of nuclei applied in this work allows for evaluation of the isotope effect.

Table 1. Calculated and Experimental Chemical Shifts of Carbon Nuclei and of the H-bonded Proton/Deuteron in PANO (in ppm), for Both Solvents[a]

	chloroform					acetonitrile				
		quantum averaged		experimental			quantum averaged		experimental	
nucleus	plain calcd	H	D	H	D	plain calcd	H	D	H	D
C(1)	148.792	147.007	147.410	138.70	138.93	149.146	147.297	147.671	139.93	140.11
C(2)	137.728	137.433	137.573	129.56	129.62	138.584	138.408	138.533	130.77	130.81
C(3)	135.973	138.821	138.172	130.68	130.23	136.896	140.340	139.694	133.10	132.57
C(4)	139.338	138.753	138.875	128.96	129.02	139.369	138.693	138.787	129.94	129.98
C(5)	146.858	145.771	145.749	137.23	137.16	146.570	145.063	145.040	137.91	137.88
C(6)	170.679	171.470	171.498	160.90	160.77	171.273	172.439	172.465	162.35	162.33
H/D	15.299	18.497	17.866	17.895	17.419	15.352	19.079	18.570	18.569	17.788

[a]The label "H" refers to the species involving a proton in the hydrogen bond, while "D" refers to the species with a deuteron. The "plain calcd" columns correspond to plain single-point B3LYP/6-311+G(2d,2p) calculations of chemical shifts using the B3LYP/6-31+G(d,p) optimized geometry within the solvent reaction field of the corresponding solvent. The "quantum averaged" columns list the thermally averaged expectation values of chemical shift functions using both proton and deuteron wave functions (see text for the details about this calculation) at 298 K.

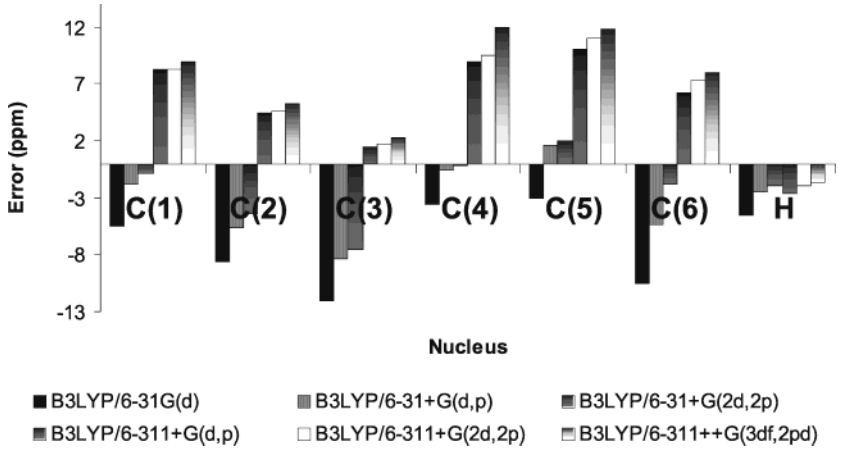

Figure 5. Comparison among the absolute values of chemical shifts in PANO, calculated by using the B3LYP density functional and several basis sets. A B3LYP/6-31+G(d,p) optimized geometry was used. No reaction field model was applied in these calculations. The values of chemical shifts are displayed as differences ("error") between the calculated and experimental (chloroform solution) values for each of the corresponding atoms.

Table 2. Calculated and Experimental Primary (H-Bonded Hydrogen) and Secondary (^{13}C) Isotope Effects $\delta_H - \delta_D$ (in ppm) in PANO in Chloroform and Acetonitrile Solution

	chloroform		acetonitrile	
nucleus	calculated	experimental	calculated	experimental
H	0.631	0.476	0.509	0.781
C(1)	−0.403	−0.23	−0.374	−0.18
C(2)	−0.140	−0.06	−0.125	−0.04
C(3)	0.649	0.47	0.646	0.53
C(4)	−0.122	−0.06	−0.094	−0.04
C(5)	0.022	0.07	0.023	0.03
C(6)	−0.028	0.13	−0.026	0.02

Table 3. Calculated and Experimental Solvent Effects ($\delta_{Acetonitrile} - \delta_{Chloroform}$; in ppm) on the Chemical Shifts of Carbon and H-Bonded Hydrogen Nuclei in PANO (for Explanation of the Column Headings, See Table 1)

		quantum averaged		experimental	
nucleus	plain calcd	H	D	H	D
C(1)	0.354	0.290	0.261	1.23	1.18
C(2)	0.856	0.975	0.960	1.21	1.19
C(3)	0.923	1.519	1.522	2.42	2.36
C(4)	0.031	−0.060	−0.088	0.98	0.96
C(5)	−0.288	−0.708	−0.709	0.68	0.72
C(6)	0.594	0.969	0.967	1.45	1.56
H/D	0.053	0.582	0.704	0.674	0.369

5. Conclusions

We calculated the chemical shifts of the H-bonded hydron and the carbon nuclei in picolinic acid *N*-oxide. Apart from the plain chemical shift calculations on the geometry-optimized structure, we constructed the two-dimensional free energy and chemical shift hypersurfaces along the O−H and O···O internal coordinates that are of major importance for the structure and dynamics of hydrogen bonding in PANO. We calculated the anharmonic vibrational wave functions and their energies and used them in the thermal quantum averaging of the chemical shift functions. With minor exceptions, we found fair agreement between the calculated and experimental chemical shifts, especially for the relative values, signs, and trends of the solvent effect and the isotope effects on chemical shifts. In particular we found a good match between the experiment and the absolute values for the primary isotope effect. Some of the calculated values are in rather poor agreement with the experiment; this can possibly be attributed to limitations of the applied methods, including the B3LYP functional, the reaction field model, and the limited number of vibrational degrees of freedom taken into account. The extensive comparison of methods for the calculation of NMR chemical shifts by Gregor, Mauri, and Car[2] offers some interesting suggestions for improvement of the present approach, for instance, calculations based on the plane-wave formalism. We also believe that the explicit solvent treatment using a QM/MM scheme would improve the results. Our experiment and calculations yield evidence that the hydron

distribution in the hydrogen bond has a significant influence on the chemical shifts of all the carbon atoms in the investigated compound.

Acknowledgment. A.J. is grateful to the Slovenian National NMR Center-Euoropean Center of Excellence (Contract Number ICA1-CT-2000-70034) for financial support and allocated instrument time. We would like to thank Prof. Albert Mildvan, The Johns Hopkins University School of Medicine for many stimulating discussions and critical reading of the manuscript. We also would like to thank Ms. Silva Zagorc and Mr. Aleksander Gačeša for their assistance in the experimental part.

JA021345F